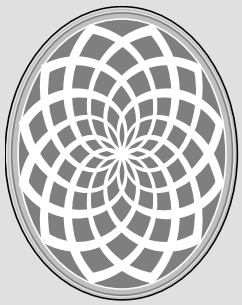


# Interdisciplinary Mathematics Institute

2013:07


# Irregular Sampling of Band-Limited Functions on the Sphere and in More General Settings


K. Ivanov and P. Petrushev



IMI

Preprint Series

College of Arts and Sciences

University of South Carolina

# IRREGULAR SAMPLING OF BAND-LIMITED FUNCTIONS ON THE SPHERE AND IN MORE GENERAL SETTINGS

KAMEN IVANOV AND PENCHO PETRUSHEV

Abstract. An iterative algorithm for stable and accurate reconstruction of band-limited functions from irregular samples on the unit 2-d sphere and the general framework of Dirichlet spaces is developed. Geometric rate of convergence in the uniform norm is achieved. It is shown that a MATLAB realization of this algorithms can effectively recover high degree ($\geq 2000$) spherical polynomials from their values at sufficiently dense scattered points on the sphere.

## 1. Introduction

In this article we consider the problem for irregular sampling of high degree spherical polynomials (band-limited functions) on the unit 2-d sphere $\mathbb{S}^2$ in $\mathbb{R}^3$. More explicitly, denoting by $\Pi_N$ the set of all spherical polynomials of degree $N$, we focus on the following

**Problem 1.** Given a finite set $Y$ of irregular sampling points on the sphere $\mathbb{S}^2$ and the values $f(y)$, $y \in Y$, of a spherical polynomial $f \in \Pi_N$ compute to prescribed accuracy $\varepsilon$ the values $f(z)$ at the points $z$ of an *arbitrary* set $Z \subset \mathbb{S}^2$.

Of course, this problem has a solution only if the density of sampling points is sufficiently high. Our main goal is to devise a fast and stable algorithm for solving Problem 1 with prescribed accuracy measured in the uniform norm, in the case when $N$ is of magnitude 1000 or higher.

Our idea is to split this problem into two:

**Problem 2.** Given the irregular sampling values $f(y)$, $y \in Y$, of a spherical polynomial $f \in \Pi_N$ compute to prescribed accuracy $\varepsilon$ its values $f(\xi)$ at *regular* grid points $\xi \in \mathcal{X} \subset \mathbb{S}^2$.

**Problem 3.** Given the values $f(\xi)$ of a spherical polynomial $f \in \Pi_N$ at regular grid points $\xi \in \mathcal{X}$ compute to prescribed accuracy $\varepsilon$ the values $f(z)$ at the points $z$ of an *arbitrary* set $Z \subset \mathbb{S}^2$.

The notion of a set $\mathcal{X}$ of *regular grid points* needs clarification. In the periodic case, $\mathcal{X}$ would be a set of uniformly distributed points. A set $\mathcal{X} \subset \mathbb{S}^2$ will be deemed regular if the values $f(\xi)$, $\xi \in \mathcal{X}$, of any polynomial $f \in \Pi_N$ allow for fast and accurate evaluation of $f(z)$ at the points $z$ of an arbitrary set $Z \subset \mathbb{S}^2$. Necessarily the cardinality $|\mathcal{X}|$ of $\mathcal{X}$ must be bigger than $(N+1)^2$. We shall utilize product-type sets of regular grid points based on 1-d uniformly distributed points

2000 *Mathematics Subject Classification.* 65T99, 42C10, 33C55, 65D15, 65D32.

*Key words and phrases.* spherical harmonics, irregular sampling, band-limited functions on the sphere, needlets, fast computation.

The first author has been supported by grant DDVU 02/30 of the Fund for Scientific Research of the Bulgarian Ministry of Education and Science. The second author has been supported by NSF Grant DMS-1211528.

and 1-d Gaussian points in spherical coordinates. The notion of a set of regular grid points on $\mathbb{S}^2$ will be further precised in Sections 3 and 4.

Traditionally, to reconstruct a spherical polynomial means to compute its spherical harmonic coefficients, see e.g. [9, 11, 12]. Unlike the trigonometric case, however, currently there are no satisfactory practical algorithms (like FFT) for fast, stable and accurate evaluation of high degree ($\geq 2000$) spherical polynomials. (The problem here is with the evaluation of the associated Legendre functions.) This is our motivation for putting forward and utilizing the following principle:

*A spherical polynomial $f \in \Pi_N$ is better represented (reconstructed) by its values $f(\xi)$ at regular grid points $\xi \in \mathcal{X}$ rather than by its spherical harmonics coefficients.*

This article is devoted to the solution of Problem 2. We develop an iterative method based on ideas from [2, 3, 4, 5] employing discrete, reproducing $\Pi_N$, operators of the form

$$\Phi_N f(x) = \sum_{\xi \in \mathcal{X}} w_\xi \mathcal{K}_N(x \cdot \xi) f(\xi), \tag{1.1}$$

which rely on highly localized kernels (spherical needlets) $\mathcal{K}_N(x \cdot \xi)$, and their truncated versions:

$$\Phi_{N,\delta} f(x) = \sum_{\substack{\xi \in \mathcal{X} \\ \rho(x,\xi) \leq \delta}} w_\xi \mathcal{K}_N(x \cdot \xi) f(\xi). \tag{1.2}$$

Here $x \cdot \xi$ stands for the inner product of $x, \xi \in \mathbb{R}^3$ and $\rho(\cdot, \cdot)$ denotes the geodesic distance on $\mathbb{S}^2$. The rate of convergence of the algorithm is geometric, measured in the uniform norm.

A fast, stable and memory efficient solution of Problem 3 based on operators $\Phi_N$ and $\Phi_{N,\delta}$ as above is given in [8].

In this article, we put the emphasis on the computational feasibility and practical realization of the algorithms. Robust MATLAB code realizing our algorithm for solving Problem 2 is developed and examples of effective reconstruction of high degree ($\geq 2000$) spherical polynomials from irregular sampling values are demonstrated.

To put our ideas and methods in prospective we develop algorithms for solving Problems 2 and 3 and hence Problem 1 in the general framework of Dirichlet spaces, developed in [1, 10]. This allows us to extend the sampling theory to various geometric settings, including irregular sampling of polynomials on the ball and simplex with weights and sampling of band-limited functions on Lie groups or homogeneous spaces with polynomial volume growth, complete Riemannian manifolds with Ricci curvature bounded from below and satisfying the volume doubling condition.

There is a considerable body of work on sampling. We find, however, suitable to only exhibit the connections between our sampling algorithm and the relevant algorithms in the literature. As already mentioned our reconstruction algorithm borrows from [2, 3, 4, 5]. The main distinction between our approach to sampling and the one in these papers is in our usage of discrete operators as in (1.2) with highly localized kernels and the recovery of the functions at regular grid points. In [6] the authors develop iterative sampling algorithms for band-limited functions on Riemannian manifolds. These are essentially theoretical $L^2$-results which extend the results from [2, 3, 4, 5]. In contrast, in our sampling algorithm the control on the error is in the uniform norm (in $L^\infty$).

In [9, 11, 12] the authors apply a least squares approach to the problem for reconstruction of spherical polynomials from scattered sample values. The proposed algorithm recovers the spherical harmonics coefficients of the polynomials. However, it requires dealing with high order associated Legendre functions, which creates instability. The practical feasibility of this algorithm is problematic when applied to point-wise evaluation of high degree ($\geq 2000$) spherical polynomials. In addition, as will be explained in Remark 4.4 below, to work properly the algorithm from [9, 11, 12] requires much denser sets of scattered points on $\mathbb{S}^2$ compared with our algorithm.

The paper is organized as follows. In §2 we develop a sampling algorithm for band-limited functions in the general setting of Dirichlet spaces. In §3 we make the needed preparations for developing our algorithm for reconstruction of spherical polynomials from irregular samples. This algorithm is given in §4. A detailed description of the software realization of our sampling algorithm on the sphere along with examples are given in §5 and §6.

We will denote by $c$ positive constants which may vary at every appearance and by $c_1, c_2, c_\diamond, C^\star$ and the alike positive constants which preserve their values throughout the paper. For a finite set $E$ we denote by $|E|$ the number of its elements.

## 2. Irregular sampling of band-limited functions in Dirichlet spaces

Although the main purpose of this article is to develop an algorithm for irregular sampling of band-limited functions on the 2-d sphere $\mathbb{S}^2 \subset \mathbb{R}^3$ we would like to put our method in a general framework which allows to cover various other settings such as on the ball and simplex with weights and on more general Riemannian manifolds and Lee groups. We believe that such a natural framework is the one of Dirichlet spaces, developed and utilized in [1, 10]. In this section we rapidly introduce this setting and put forward the main ideas.

### 2.1. **The setting.**

There are two sets of conditions that we now describe briefly:

I. We assume that $(\mathcal{M}, \rho, \mu)$ is a metric measure space satisfying the conditions: $(\mathcal{M}, \rho)$ is a locally compact metric space with distance $\rho(\cdot, \cdot)$ and $\mu$ is a positive Radon measure such that the following *volume doubling condition* is valid

$$0 < \mu(B(x, 2r)) \leq c_0 \mu(B(x, r)) < \infty \quad \text{for all } x \in \mathcal{M} \text{ and } r > 0, \tag{2.1}$$

where $B(x, r)$ is the open ball centered at $x$ of radius $r$ and $c_0 > 1$ is a constant.

Note that (2.1) readily implies

$$\mu(B(x, \lambda r)) \leq c_0 \lambda^d \mu(B(x, r)) \quad \text{for } x \in \mathcal{M},\ r > 0, \text{ and } \lambda > 1. \tag{2.2}$$

Here $d = \log_2 c_0 > 0$ is a constant.

II. The main assumption is that the space $(\mathcal{M}, \rho, \mu)$ is related to an essentially self-adjoint positive operator $L$ on $L^2(\mathcal{M}, d\mu)$ such that the associated semigroup $P_t = e^{-tL}$ consists of integral operators with (heat) kernel $p_t(x, y)$ obeying the conditions:

- *Small time Gaussian upper bound*:

$$|p_t(x, y)| \leq \frac{C^\star \exp\{-\frac{c^\star \rho^2(x,y)}{t}\}}{\sqrt{\mu(B(x, \sqrt{t}))\mu(B(y, \sqrt{t}))}} \quad \text{for } x, y \in \mathcal{M},\ 0 < t \leq 1. \tag{2.3}$$

- *Hölder continuity*: There exists a constant $\beta > 0$ such that

$$|p_t(x,y) - p_t(x,y')| \le C^\star \Big(\frac{\rho(y,y')}{\sqrt{t}}\Big)^\beta \frac{\exp\{-\frac{c^\star \rho^2(x,y)}{t}\}}{\sqrt{\mu(B(x,\sqrt{t}))\mu(B(y,\sqrt{t}))}} \tag{2.4}$$

for $x, y, y' \in M$ and $0 < t \le 1$, whenever $\rho(y,y') \le \sqrt{t}$.

- *Markov property*:

$$\int_{\mathcal{M}} p_t(x,y) d\mu(y) \equiv 1 \quad \text{for } t > 0. \tag{2.5}$$

Above $C^\star, c^\star > 0$ are structural constants.

We also assume the following *non-collapsing condition*:

$$\inf_{x\in\mathcal{M}} \mu(B(x,1)) > 0. \tag{2.6}$$

A natural effective realization of the above setting appears in the general framework of Dirichlet spaces. More precisely, in the framework of *strictly local regular Dirichlet spaces with a complete intrinsic metric* it suffices to only verify

(1) the local Poincaré inequality and
(2) the global doubling condition on the measure (2.1)

and then the above general setting applies in full, see [1]. The point is that settings where our theory applies are quite common. In particular, the sphere, ball and simplex with classical weights are covered. Various other examples are given in [1].

2.2. **Spectral spaces.** Let $E_\lambda$, $\lambda \ge 0$, be the spectral resolution associated with the self-adjoint positive operator $L$ from above on $L^2(\mathcal{M}, d\mu)$. We let $F_\lambda$, $\lambda \ge 0$, denote the spectral resolution associated with $\sqrt{L}$, i.e. $F_\lambda = E_{\lambda^2}$. Then for any measurable and bounded function $\phi$ on $\mathbb{R}_+$ the operator $\phi(\sqrt{L})$ is defined by $\phi(\sqrt{L}) = \int_0^\infty \phi(\lambda) dF_\lambda$ on $L^2(\mathcal{M}, d\mu)$. For any $N > 0$ the $L^\infty$ spectral space $\Sigma_N$ is defined by

$$\Sigma_N := \big\{ f \in C(\mathcal{M}) : \phi(\sqrt{L}) f = f \text{ for all } \phi \in C_0^\infty(\mathbb{R}_+),\ \phi \equiv 1 \text{ on } [0,N] \big\}. \tag{2.7}$$

Here $C_0^\infty(\mathbb{R}_+)$ denotes the set of all compactly supported $C^\infty$ functions on $\mathbb{R}_+$.

2.3. **Almost exponentially localized reproducing kernels (father needlets).** Well localized reproducing kernels for band limited functions will be the main vehicle in designing a sampling algorithm in the general setting described in §2.1.

Let $\varphi \in C^\infty(\mathbb{R}_+)$ be a cut-off function so that

$$\varphi(t) = 1,\ t \in [0,1];\ 0 \le \varphi(t) \le 1,\ t \in [1, 1+\tau]; \varphi(t) = 0,\ t \ge 1+\tau \tag{2.8}$$

for some $\tau > 0$. As shown in [1, 10] the operator $\varphi(N^{-1}\sqrt{L})$ with $N > 0$ is an integral operator, i.e.

$$\varphi(N^{-1}\sqrt{L}) f(x) = \int_{\mathcal{M}} \mathcal{K}_N(x,y) f(y) d\mu(y). \tag{2.9}$$

From Spectral Theory it follows that for a real-valued $\varphi$ the kernel $\mathcal{K}_N(x,y)$ is symmetric: $\overline{\mathcal{K}_N(y,x)} = \mathcal{K}_N(x,y)$ and for every fixed $x$ belongs to $\Sigma_{(1+\tau)N}$. More importantly, the kernel $\mathcal{K}_N(x,y)$ has almost exponential localization and Hölder

continuity [10]: *For any $\sigma > 0$ there exists a constant $c'_\sigma > 0$ such that for any $N > 0$*

$$|\mathcal{K}_N(x,y)| \le \frac{c'_\sigma}{\mu(B(x,N^{-1}))(1+N\rho(x,y))^\sigma}, \quad x,y \in M, \tag{2.10}$$

*and*

$$|\mathcal{K}_N(x,y) - \mathcal{K}_N(x',y)| \le \frac{c'_\sigma \big(N\rho(x,x')\big)^\beta}{\mu(B(y,N^{-1}))(1+N\rho(x,y))^\sigma} \ \text{ if } \rho(x,x') \le N^{-1}. \tag{2.11}$$

*Here $\beta > 0$ is the constant from* (2.4).

Note that for a cut-off function $\varphi$ with "small derivatives" the kernel $\mathcal{K}_N(x,y)$ may have sub-exponential localization, see [10, Theorem 3.6].

Our next step is to derive a discrete version of the operator $\varphi(N^{-1}\sqrt{L})$ in the case when the spectral spaces $\Sigma_N$ possess the *polynomial property*:

$$\Sigma_K \cdot \Sigma_N \subset \Sigma_{K+N}, \quad \text{i.e.} \quad f \in \Sigma_K, g \in \Sigma_N \Longrightarrow fg \in \Sigma_{K+N}. \tag{2.12}$$

This is the case when the eigenfunctions of the operator $L$ are polynomials such as in the case of the sphere, ball, and simplex with classical weights.

An important component of our scheme is the existence of cubature formulae on $\mathcal{M}$ involving convenient *regular grid points* (*nodes*). Namely, we assume that given $N \ge 1$ and $\tau > 0$ there exists a finite or countable set $\mathcal{X} \subset \mathcal{M}$ and a set of positive weights $\{w_\xi\}_{\xi\in\mathcal{X}}$ such that

$$\int_{\mathcal{M}} f(y)d\mu(y) = \sum_{\xi\in\mathcal{X}} w_\xi f(\xi) \quad \forall f \in \Sigma_{(2+\tau)N}. \tag{2.13}$$

Moreover, we assume that there exists a companion to $\mathcal{X}$ disjoint partition $\{\mathcal{D}_\xi\}_{\xi\in\mathcal{X}}$ of $\mathcal{M}$ ($\mathcal{M} = \cup_{\xi\in\mathcal{X}}\mathcal{D}_\xi$) consisting of measurable sets such that

$$\mathcal{D}_\xi \subset B(\xi, c_1N^{-1}) \quad \text{and} \quad w_\xi \le c_2\mu(\mathcal{D}_\xi), \quad \xi \in \mathcal{X}, \tag{2.14}$$

where $c_1, c_2 > 0$ are constants.

Observe that conditions (2.14) are not quite restrictive and allow us the freedom to choose convenient cubature formulae. The existence of cubature formulae in our general setting follows by [1, Theorem 4.4].

The following lemma will be instrumental in our further development.

**Lemma 2.1.** *Let $N \ge 1$ and $\tau > 0$. Assume $\mathcal{X}$ is the set of nodes of the cubature formula from* (2.13) *such that the companion to $\mathcal{X}$ disjoint partition $\{\mathcal{D}_\xi\}_{\xi\in\mathcal{X}}$ satisfies* (2.14). *Then for any $\sigma > d$ with $d > 1$ the constant from* (2.2) *there exists a constant $\bar{c}_\sigma > 0$ such that*

$$\sum_{\xi\in\mathcal{X}} \frac{w_\xi}{\mu(B(\xi,N^{-1}))\big(1+N\rho(x,\xi)\big)^\sigma} \le \bar{c}_\sigma \quad \forall x \in \mathcal{M}. \tag{2.15}$$

*Proof.* Set $\gamma := c_1N^{-1}$, where $c_1 > 0$ is the constant from (2.14). Let $\mathcal{T}$ be a maximal $\gamma$-net on $\mathcal{M}$, that is, $\rho(t,u) \ge \gamma$ for all $t,u \in \mathcal{T}$ and $\mathcal{T}$ cannot be enlarged. By Zorn's lemma it follows that a maximal $\gamma$-net $\mathcal{T}$ exists. Moreover $\mathcal{T}$ is finite or countable (see [1, Proposition 2.5]). Furthermore, we have

$$M = \cup_{t\in\mathcal{T}} B(t,\gamma) \quad \text{and} \quad B(t,\gamma/2) \cap B(u,\gamma/2) = \emptyset \ \text{ for } t,u \in \mathcal{T},\ t \ne u. \tag{2.16}$$

Now, we split $\mathcal{X}$ into disjoint subsets $\mathcal{X}(t)$ , $t\in\mathcal{T}$, so that $\xi\in B(t,\gamma)$ if $\xi\in\mathcal{X}(t)$. We claim that

(2.17)
$$\sum_{\xi\in\mathcal{X}(t)}\frac{w_\xi}{\mu(B(\xi,N^{-1}))\big(1+N\rho(x,\xi)\big)^\sigma}\le\frac{c}{\big(1+\gamma^{-1}\rho(x,t)\big)^\sigma},\quad x\in\mathcal{M},\ t\in\mathcal{T}.$$

Indeed, clearly for any $\xi\in\mathcal{X}(t)$ (hence $\rho(\xi,t)<\gamma$) and $x\in\mathcal{M}$ we have

$$1+\gamma^{-1}\rho(x,t)\le 1+\gamma^{-1}\rho(x,\xi)+\gamma^{-1}\rho(\xi,t)\le 2+c_1^{-1}N\rho(x,\xi)\le c(1+N\rho(x,\xi)).$$

Also, clearly $B(t,\gamma)\subset B(\xi,2\gamma)$ and hence

$$\mu(B(t,\gamma))\le\mu(B(\xi,2c_1N^{-1}))\le c\mu(B(\xi,N^{-1})),$$

where for the last inequality we used (2.2). Furthermore, using (2.14) we have

$$\cup_{\xi\in\mathcal{X}(t)}\mathcal{D}_\xi\subset\cup_{\xi\in\mathcal{X}(t)}B(\xi,\gamma)\subset B(t,2\gamma)$$

and hence

$$\sum_{\xi\in\mathcal{X}(t)}w_\xi\le c_2\sum_{\xi\in\mathcal{X}(t)}\mu(\mathcal{D}_\xi)=c_2\mu\left(\cup_{\xi\in\mathcal{X}(t)}\mathcal{D}_\xi\right)\le c_2\mu(B(t,2\gamma))\le c\mu(B(t,\gamma)).$$

Putting the above together, we obtain (2.17).

In turn, (2.17) implies that (2.15) will be valid if we show that for any $\sigma>d$

$$\sum_{t\in\mathcal{T}}\frac{1}{\big(1+\gamma^{-1}\rho(x,t)\big)^\sigma}\le c<\infty,\quad x\in\mathcal{M}. \tag{2.18}$$

To prove this, fix $x\in\mathcal{M}$ and put

$$\mathcal{S}_0:=\{t\in\mathcal{T}:\rho(x,t)<2^{-1}\gamma\}\text{ and }\mathcal{S}_j:=\{t\in\mathcal{T}:2^{j-2}\gamma\le\rho(x,t)<2^{j-1}\gamma\},\ j\ge1.$$

For any $u\in\mathcal{S}_j$, clearly, $\cup_{t\in\mathcal{S}_j}B(t,\gamma/2)\subset B(x,2^j\gamma)\subset B(u,2^{j+1}\gamma)$ and taking into account (2.16)

$$\sum_{t\in\mathcal{S}_j}\mu(B(t,\gamma/2))=\mu\left(\cup_{t\in\mathcal{S}_j}B(t,\gamma/2)\right)\le\mu(B(u,2^{j+1}\gamma))\le c2^{jd}\mu(B(u,\gamma/2)),$$

where for the last inequality we used (2.2). Summing up both sides of the above inequalities over $u\in\mathcal{U}_j$ yields $|\mathcal{S}_j|\le c2^{jd}$, implying

$$\begin{aligned}\sum_{t\in\mathcal{T}}\frac{1}{\big(1+\gamma^{-1}\rho(x,t)\big)^\sigma}&=\sum_{j=0}^\infty\sum_{t\in\mathcal{S}_j}\frac{1}{\big(1+\gamma^{-1}\rho(x,t)\big)^\sigma}\\&\le 1+\sum_{j=1}^\infty\frac{|\mathcal{S}_j|}{(1+2^{j-2})^\sigma}\le c\sum_{j=0}^\infty 2^{-(\sigma-d)j}\le c<\infty,\end{aligned}$$

which verifies (2.18). □

Armed with the cubature formula from (2.13) we define

$$\Phi_Nf(x):=\sum_{\xi\in\mathcal{X}}w_\xi\mathcal{K}_N(x,\xi)f(\xi). \tag{2.19}$$

For $f\in\Sigma_N$ we have by (2.12) $\mathcal{K}_N(x,\cdot)f(\cdot)\in\Sigma_{(2+\tau)N}$ for any fixed $x\in\mathbb{S}^2$. Then using that the cubature formula from (2.13) is exact for functions from $\Sigma_{(2+\tau)N}$ and (2.7) with $\phi(\cdot)=\varphi(\cdot/N)$ we get

$$\Phi_Nf=f\quad\text{for}\quad f\in\Sigma_N. \tag{2.20}$$

Note that the construction of discrete reproducing operators $\Phi_N$ is also possible in the case when the spectral spaces $\Sigma_N$ do not possess the polynomial property (2.12). The existence of such operators follows by Lemma 4.2 in [10], used for construction of dual frames in [10]. We shall not elaborate on this since in this study our focus is on the case of the sphere where (2.12) is valid.

2.4. **Irregular sampling: The general idea.** We next focus on the irregular sampling problem for reconstruction of band-limited functions in the general setting described in §2.1. Namely, we consider **Problem 1** for fast and accurate evaluation of a band-limited function $f \in \Sigma_N$ on an arbitrary set of scattered points $Z \subset \mathcal{M}$ given its values on a set of irregular sampling points $Y \subset \mathcal{M}$.

Just as in the introduction we subdivide this problem into two: **Problem 2** for recovery the values of $f \in \Sigma_N$ at regular grid points $\xi \in \mathcal{X}$ from its values at irregular sampling points $y \in Y$, and **Problem 3** for computing the values of $f \in \Sigma_N$ at arbitrary points $z \in Z$ given its values at regular grid points $\xi \in \mathcal{X}$.

We shall show that Problem 2 can be effectively solved if the given set $Y \subset \mathcal{M}$ of sampling points is an $\epsilon$-cover for $\mathcal{M}$ for sufficiently small $\epsilon$.

To describe the solution of Problem 2, we assume that given the set $Y \subset \mathcal{M}$ of sampling points there is a companion disjoint partition $\mathcal{A} = \{A_y\}_{y\in Y}$ of $\mathcal{M}$ ($\mathcal{M} = \cup_{y\in Y} A_y$) consisting of measurable sets such that

$$d(\mathcal{A}) := \sup_{y\in Y} \sup_{x\in A_y} \rho(x,y) < \infty. \tag{2.21}$$

Given $x \in \mathcal{M}$ denote by $y_x$ the point in $Y$ such that $x \in A_{y_x}$. We introduce the following extension operator for functions $g$ defined on $Y$:

$$\mathcal{E}_{\mathcal{A}} g(x) := \sum_{y\in Y} g(y) \mathbb{1}_{A_y}(x) = g(y_x), \quad x \in \mathcal{M}, \tag{2.22}$$

where $\mathbb{1}_{A_y}$ is the characteristic function of $A_y$.

We also assume that $\mathcal{X} \subset \mathcal{M}$ is a regular set as in §2.3 with associated cubature formula (2.13) and reproducing operator $\Phi_N$ as in (2.19).

The solution of Problem 2 is contained in the following

**Theorem 2.1.** *For some $\sigma > d$ with $d > 1$ the constant from (2.2) and $0 < q < 1$ assume*

$$d(\mathcal{A}) \le c_\diamond N^{-1}, \quad c_\diamond := \min\{1, (q/(c'_\sigma \bar{c}_\sigma))^{1/\beta}\}, \tag{2.23}$$

*where $\beta$ and $c'_\sigma$ are from (2.11) and $\bar{c}_\sigma$ is from (2.15). Set $\mathcal{R} := (\mathcal{I} - \mathcal{E}_A)\Phi_N$, where $\mathcal{I}$ is the identity. Then for any $f \in \Sigma_N$ we have*

$$f = \sum_{k=0}^{\infty} \mathcal{R}^k(\mathcal{E}_A f) \tag{2.24}$$

*with the series converging uniformly and*

$$\big\| f - \sum_{k=0}^{n-1} \mathcal{R}^k(\mathcal{E}_A f) \big\|_\infty \le q^n \|f\|_\infty, \quad n \ge 1. \tag{2.25}$$

*Proof.* For any $x \in \mathcal{M}$ and for any $f \in L^\infty(\mathcal{M})$ we have

$$\mathcal{R}f(x) = \Phi_N f(x) - \Phi_N f(y_x) = \sum_{\xi\in\mathcal{X}} w_\xi \big[\mathcal{K}_N(x,\xi) - \mathcal{K}_N(y_x,\xi)\big] f(\xi)$$

and using (2.11) with $\sigma > d$ and Lemma 2.1 we infer

$$|\mathcal{R}f(x)| \le c'_\sigma \big(Nd(\mathcal{A})\big)^\beta \sum_{\xi\in\mathcal{X}} \frac{w_\xi}{\mu(B(\xi,N^{-1}))\big(1+N\rho(x,\xi)\big)^\sigma}\|f\|_\infty \le c'_\sigma \bar{c}_\sigma c_\diamond^\beta \|f\|_\infty.$$

Therefore, $\|\mathcal{R}f\|_\infty \le q\|f\|_\infty$.

Now, let $f \in \Sigma_N$. In view of (2.20) $\Phi_N f = f$, hence $\mathcal{R}f = f - \mathcal{E}_A f$ and for $k \ge 1$

$$\mathcal{R}^k f - \mathcal{R}^{k+1} f = \mathcal{R}^k(f - \mathcal{R}f) = \mathcal{R}^k(\mathcal{E}_A f).$$

This leads to

$$f - \sum_{k=0}^{n-1} \mathcal{R}^k(\mathcal{E}_A f) = \mathcal{R}^n f$$

and using that $\|\mathcal{R}\|_{\infty\mapsto\infty} \le q < 1$ we arrive at (2.25), which in turn implies (2.24). □

**Algorithm for solving Problem 2.** Given the values $f(y)$, $y \in Y$, of a band-limited function $f \in \Sigma_N$ we would like to compute $f(\xi)$ for $\xi \in \mathcal{X}$. Denote briefly $g_k := \mathcal{R}^k(\mathcal{E}_A f)$. Then by (2.24) we have

$$f(\xi) = \sum_{k=0}^{\infty} g_k(\xi), \quad \xi \in \mathcal{X}. \tag{2.26}$$

A key point is that the values $g_k(\xi)$, $\xi \in \mathcal{X}$, can be computed iteratively. Namely, we first compute $g_0(\xi) = \mathcal{E}_A f(\xi) = f(y_\xi)$, $\xi \in \mathcal{X}$, and in the next step

$$g_1(\xi) = \mathcal{R}g_0(\xi) = \Phi_N g_0(\xi) - \Phi_N g_0(y_\xi),$$

where for the computation of the values $\Phi_N g_0(\xi)$ we only use $g_0(\eta)$, $\eta \in \mathcal{X}$. The general step is

$$g_{k+1}(\xi) = \mathcal{R}g_k(\xi) = \Phi_N g_k(\xi) - \Phi_N g_k(y_\xi)$$

and we observe again that to compute $g_{k+1}(\xi)$ we only need $g_k(\eta)$, $\eta \in \mathcal{X}$. Of course, we replace the series in (2.26) by a finite sum

$$f(\xi) \approx \sum_{k=0}^{n} g_k(\xi), \quad \xi \in \mathcal{X},$$

where because of (2.25) the convergence is geometric and we have complete control on the error.

To make the above algorithms computationally efficient we use the superb localization of the kernel $\mathcal{K}_N(x,\xi)$ to truncate the operator $\Phi_N f$ from (2.19). Namely, we replace it by the operator

$$\Phi_{N,\delta} f(x) = \sum_{\substack{\xi\in\mathcal{X}\\ \rho(x,\xi)\le\delta}} w_\xi \mathcal{K}_N(x,\xi) f(\xi), \tag{2.27}$$

with appropriately selected constant $\delta$.

The utilization of the operator $\Phi_{N,\delta}$ with a kernel of small support opens the possibility of using simultaneously more than one regular sets $\mathcal{X}$. The point is that part of the nodes in a particular regular set $\mathcal{X}$ are usually not quite well distributed, which creates problems. This inconvenience can be overcome by using two or more different regular sets $\mathcal{X}$ for different subregions of $\mathcal{M}$.

An effective implementation of the above algorithm for irregular sampling of band-limited functions on the sphere $\mathbb{S}^2 \subset \mathbb{R}^3$ with a thorough analysis of its features: accuracy, complexity, and computational efficiency, and a description of the relevant software are given in what follows.

**Algorithm for solving Problem 3.** Once we have the values of the band limited function $f \in \Sigma_N$ at the regular points $\xi \in \mathcal{X}$ we use that $\Phi_N f = f$ and (2.19) to compute $f(z)$, $z \in Z$, i.e.

$$f(z) = \sum_{\xi \in \mathcal{X}} w_\xi \mathcal{K}_N(z, \xi) f(\xi), \quad z \in Z.$$

For computational efficiency we again replace the operator $\Phi_N$ by its truncated version $\Phi_{N,\delta}$, see (2.27). For a complete analysis of this algorithm and implementation on the sphere $\mathbb{S}^2 \subset \mathbb{R}^3$ we refer the reader to [8].

## 3. Sampling of band-limited functions on the sphere: Preparation

Our main focus is on irregular sampling of band-limited functions on the 2-d sphere $\mathcal{M} = \mathbb{S}^2 \subset \mathbb{R}^3$. The metric $\rho(x, y) = \arccos(x \cdot y)$ with $x \cdot y$ denoting the inner product in $\mathbb{R}^3$ is in fact the geodesic distance on $\mathbb{S}^2$, the measure is $d\mu = (4\pi)^{-1} d\sigma$, where $\sigma$ is the Lebesgue measure on $\mathbb{S}^2$, and the spectral space $\Sigma_N$ is $\Pi_N$ – the set of all spherical polynomials (band-limited functions) of degree $\leq N$.

The present section lays down some of the ground work that will be needed for developing our sampling algorithm on the sphere.

3.1. **Regular point sets on the sphere.** Given $M \in \mathbb{N}$ we say that $\mathcal{X}$ is a set of $M-$*regular* points on the sphere if the following two conditions are verified:

(1) There exist *non-negative* weights $w_\xi$, $\xi \in \mathcal{X}$, of a cubature formula with $\mathcal{X}$ as a nodal set which is exact for the polynomials from $\Pi_{M-1}$, i.e.

$$\frac{1}{4\pi} \int_{\mathbb{S}^2} f(y)\, d\sigma(y) = \sum_{\xi \in \mathcal{X}} w_\xi f(\xi) \quad \forall f \in \Pi_{M-1}, \tag{3.1}$$

and (2.14) is satisfied with $M$ in the place of $N$;

(2) The set $\mathcal{X}$ is *structured* in the sense that for every $x \in \mathbb{S}^2$ and $\delta \in (0, \pi]$ one can determine effectively all points in $\bar{B}_{\mathcal{X}}(x, \delta) = \{\xi \in \mathcal{X} : \rho(x, \xi) \leq \delta\}$ using $c|\bar{B}_{\mathcal{X}}(x, \delta)|$ operations, where the constant $c$ is independent of $x$, $\delta$, $M$ and $|\mathcal{X}|$.

Examples of regular point sets on the sphere are $\mathcal{X}^{(i)} = \{\xi_{k,\ell}^{(i)} = (\theta_k^{(i)}, \lambda_\ell^{(i)})\}$, $i = 1, 2$, that for given $K, L \geq 1$ are defined by

$$\theta_k^{(1)} = \frac{\pi}{K} k,\ k = 0, 1, \ldots, K;\ \lambda_\ell^{(1)} = \frac{2\pi}{L} \ell,\ \ell = 0, 1, \ldots, L-1;$$

and

$$\theta_k^{(2)} = \frac{\pi}{K} k - \frac{\pi}{2K},\ k = 1, 2, \ldots, K;\ \lambda_\ell^{(2)} = \frac{2\pi}{L} \ell,\ \ell = 0, 1, \ldots, L-1.$$

Here in $\mathcal{X}^{(1)}$ we consider only one node for $k = 0$ (the North Pole) and only one node for $k = K$ (the South Pole). Another example is the set $\mathcal{X}^{(3)}$ generated by the zeros $u_k$ of the $K$-th degree Legendre polynomial $P_K$. In this case we write

$$\theta_k^{(3)} = \arccos u_k,\ k = 1, 2, \ldots, K;\ \lambda_\ell^{(3)} = \frac{2\pi}{L} \ell,\ \ell = 0, 1, \ldots, L-1.$$

As is well-known the cubatures associated with $\mathcal{X}^{(1)}, \mathcal{X}^{(2)}, \mathcal{X}^{(3)}$ can be represented as tensor products of one-dimensional algebraic quadrature in the co-latitude direction $\theta$ and the rectangular trigonometric quadrature in the latitude direction (see e.g. [8, Subsection 3.4]). The relations between $K, L$ and $M$ are given by (see [8, Theorem 3.11])

$$M \le L, \qquad M \le \begin{cases} 2\lfloor (K+1)/2 \rfloor, & i = 1, 2; \\ 2K, & i = 3. \end{cases}$$

Under the above restrictions the sets $\mathcal{X}^{(1)}, \mathcal{X}^{(2)}, \mathcal{X}^{(3)}$ are $M$-regular [8, Theorems 3.11 and 3.12].

Other regular point sets can be obtained from $\mathcal{X}^{(1)}$, $\mathcal{X}^{(2)}$, or $\mathcal{X}^{(3)}$ by applying rotations or reflections on the sphere. For example, consider the map $T : \mathbb{R}^3 \to \mathbb{R}^3$ given by

$$T(x_1, x_2, x_3) = (x_1, x_3, -x_2).$$

This is $\pi/2$ rotation about the $x_1$-axis. The restriction of $T$ on the sphere $T|_{\mathbb{S}^2} : \mathbb{S}^2 \to \mathbb{S}^2$ relates the spherical coordinates $(\theta, \lambda)$ and $(\tilde{\theta}, \tilde{\lambda})$ of a point $x$ and its image $\tilde{x} = T(x)$ by

$$(\sin\tilde{\theta}\cos\tilde{\lambda}, \sin\tilde{\theta}\sin\tilde{\lambda}, \cos\tilde{\theta}) = (\sin\theta\cos\lambda, \cos\theta, -\sin\theta\sin\lambda).$$

From the rotation invariance of $\Pi_N$ it follows that the sets $T(\mathcal{X}^{(i)})$ and $T^{-1}(X^{(i)})$, $i = 1, 2, 3$, are also regular and induce similar cubatures as $\mathcal{X}^{(i)}$.

All of the above regular point sets have one disadvantage – their points congregate near the poles (or the images of the poles). This will force us later to treat the points near the poles differently compared to the ones away from the poles.

3.2. **Spherical needlets.** For the purposes of evaluation of spherical polynomials it is convenient to use spherical "father needlets" that will be defined via kernels of the form

$$\mathcal{K}_N(u) = \sum_{\nu=0}^{\infty} \varphi\Big(\frac{\nu}{N}\Big)(2\nu+1)P_\nu(u), \quad u \in [-1, 1], \tag{3.2}$$

where $P_\nu$ is the Legendre polynomial of degree $\nu$ normalized by $P_\nu(1) = 1$ and $\varphi$ is a continuous cutoff function satisfying (2.8) for some fixed $\tau > 0$.

For a set of $M-$*regular* points $\mathcal{X} \subset \mathbb{S}^2$, $M \ge \lceil (2+\tau)N \rceil$, using the weights $w_\xi$ from (3.1) we define the linear operator $\Phi_N$ by

$$\Phi_N f(x) = \sum_{\xi \in \mathcal{X}} w_\xi \mathcal{K}_N(x \cdot \xi) f(\xi). \tag{3.3}$$

Clearly, $\Phi_N f = f$ for $f \in \Pi_N$ and $\Phi_N : \ell^\infty(\mathcal{X}) \mapsto \Pi_{N_\tau}$ with

$$N_\tau = \lceil (1+\tau)N \rceil - 1. \tag{3.4}$$

The superb localization of the kernel $\mathcal{K}_N$ implies that most of the terms in (3.3) are very small and this leads us to the idea of introducing the truncated operator

$$\Phi_{N,\delta} f(x) = \sum_{\substack{\xi \in \mathcal{X} \\ \rho(x,\,\xi) \le \delta}} w_\xi \mathcal{K}_N(x \cdot \xi) f(\xi), \tag{3.5}$$

where $\delta > 0$ is a small parameter. Observe that the above sum includes only summands corresponding to nodes $\xi \in \mathcal{X}$, which are in the $\delta$-neighborhood of the point $x$.

We shall also need the rotated by $T$ versions $\tilde{\Phi}_N$, $\tilde{\Phi}_{N,\delta}$ of the operators $\Phi_N$, $\Phi_{N,\delta}$ defined in (3.3) and (3.5) with $\mathcal{X}$ replaced by $T(\mathcal{X})$, i.e.

$$\tilde{\Phi}_N f(x) = \sum_{\xi\in T(\mathcal{X})} \widetilde{w}_\xi \mathcal{K}_N(x\cdot\xi) f(\xi), \quad \tilde{\Phi}_{N,\delta} f(x) = \sum_{\substack{\xi\in T(\mathcal{X})\\ \rho(x,\xi)\le\delta}} \widetilde{w}_\xi \mathcal{K}_N(x\cdot\xi) f(\xi),$$

where $\widetilde{w}_\xi = w_{T^{-1}(\xi)}$ for $\xi \in T(\mathcal{X})$.

3.3. **Localization of spherical needlets.** In this subsection we discuss the question of how small $\delta$ in (3.5) can be in order that $\Phi_N f$ be a good approximation to $f \in \Pi_N$. The following simple claim gives the first answer (see [8, Theorem 2.4]):

**Proposition 3.1.** *If*

$$|\mathcal{K}_N(\cos\theta)| \le \varepsilon \quad \textit{for} \quad \delta \le \theta \le \pi, \tag{3.6}$$

*then for any function $f : \mathcal{X} \to \mathbb{R}$ we have*

$$\|\Phi_N f - \Phi_{N,\delta} f\|_{L_\infty(\mathbb{S}^2)} \le \varepsilon \|f\|_{\ell^\infty(\mathcal{X})}. \tag{3.7}$$

According to [8, Theorem 3.2] for any $\varepsilon > 0$ there exists a cutoff function $\varphi$ satisfying (2.8) such that (3.6) holds with

$$\delta \le c\frac{\ln(N^2) + \ln(1/\varepsilon) + \ln(1+\tau)}{\tau N}. \tag{3.8}$$

In Proposition 3.1 condition (3.6) can be replaced by

$$\frac{1}{2}\int_{-1}^{\cos\delta} |\mathcal{K}_N(u)|\,du = \varepsilon \quad \left(= \frac{\varepsilon}{2}\int_{-1}^{1} \mathcal{K}_N(u)\,du\right) \tag{3.9}$$

and still have (3.7) as an approximate inequality (see [8, (3.11)]). On account of [8, Theorem 3.6] for any $\varepsilon > 0$ there exists a cutoff function $\varphi$ obeying (2.8) such that (3.9) holds with

$$\delta \le c\frac{\ln(1/\varepsilon)}{\tau N}. \tag{3.10}$$

Estimate (3.10) is an improvement of (3.8) mainly due to the missing $\ln N$ term in the numerator. One can have $c = 2.5$ in (3.10) when working with cutoff functions $\varphi$ (satisfying (2.8)) given by

$$\varphi(t) = \kappa^{-1}\int_{(t-1)/\tau}^{1} e^{b\sqrt{v(1-v)}}\,dv, \quad \kappa = \int_0^1 e^{b\sqrt{v(1-v)}}\,dv,\ b > 0, \tag{3.11}$$

for $t$ in $[1, 1+\tau]$. In (3.11) $b$ is a parameter, which for $4 < \log_{10}(1/\varepsilon) < 11$ and $\tau \ge 1$ is given by

$$b = 4.8\log_{10}(1/\varepsilon) + 3.4 - 0.2\min\{\tau, 3\}. \tag{3.12}$$

For more details, see [8].

## 4. Sampling of band-limited functions on the sphere: Algorithm

4.1. **Formulation of the problem.** For the reader's convenience we begin by restating our version of the problem for irregular sampling of band-limited functions on the sphere.

**Problem 1.** Given a finite set $Y$ of irregular sampling points on the sphere $\mathbb{S}^2$ and the sampling values $f(y)$, $y \in Y$, of a polynomial $f \in \Pi_N$ at these points compute to prescribed accuracy $\varepsilon$ the values $f(z)$ of the polynomial $f$ at *arbitrary* points $z \in Z \subset \mathbb{S}^2$.

Our main objective is to devise a fast and stable algorithm for solving Problem 1 with prescribed accuracy measured in the uniform norm, in the case when both cardinalities $|Y|$ and $|Z|$ are larger than $\dim \Pi_N = (N+1)^2$.

Following the idea in §2.4 we split this problem into two:

**Problem 2.** Given a set of sampling points $Y \subset \mathbb{S}^2$ and the values $f(y)$ of a polynomial $f \in \Pi_N$ at the points $y \in Y$ compute to prescribed accuracy $\varepsilon$ the values $f(\xi)$ of the polynomial $f$ at the $\lceil (2+\tau)N \rceil$-*regular* points $\xi \in \mathcal{X} \subset \mathbb{S}^2$.

**Problem 3.** Given $\lceil (2+\tau)N \rceil$-*regular* point set $\mathcal{X} \subset \mathbb{S}^2$ and the values $f(\xi)$, $\xi \in \mathcal{X}$, of a polynomial $f \in \Pi_N$ compute to prescribed accuracy $\varepsilon$ the values $f(z)$ at *arbitrary* points $z \in Z \subset \mathbb{S}^2$.

Above $\tau > 0$ is the needlet parameter from (2.8).

The main input in Problem 2 are the set $Y$ and the degree $N$. We are free to chose the *regular* set $\mathcal{X}$ because after its solution we solve Problem 3 to get a solution of Problem 1 and the needlet solution of Problem 2 works with every regular point set $\mathcal{X}$.

In [8] we developed needlets based fast and stable algorithm for solving Problem 3. An *exact solution* of Problem 3 is given by $f(z) = \Phi_N f(z)$ and an *approximate solution* by $f(z) \approx \Phi_{N,\delta} f(z)$, where $\Phi_N$ and $\Phi_{N,\delta}$ are defined in (3.3) and (3.5).

In the following we focus on Problem 2.

4.2. **Exact solution of Problem 2.** Given a finite set of sampling points $Y \subset \mathbb{S}^2$ let $\mathcal{A} = \{A_y\}_{y \in Y}$ be a disjoint partition of $\mathbb{S}^2$ consisting of measurable sets $A_y$, such that $y \in A_y$.

In particular, $\{A_y\}$ can be the Voronoi tessellation of $\mathbb{S}^2$ induced by $Y$, where the common points from the boundaries of several cells are attached to exactly one of the cells. Another meaningful example are the HEALPix centers $Y$ with the pixels collected in $\{A_y\}$.

The following notation will be useful: For any $x \in \mathbb{S}^2$ we denote by $y_x$ the point in $Y$ such that $x \in A_{y_x}$. Consider the extension operator

$$\mathcal{E}_{\mathcal{A}} g(x) := \sum_{y \in Y} g(y) \mathbb{1}_{A_y}(x) = g(y_x) \tag{4.1}$$

defined for any function $g : Y \to \mathbb{R}$. Obviously $\|\mathcal{E}_{\mathcal{A}}\| = 1$ (all operator norms are $\infty \mapsto \infty$ norms). Denote

$$d(\mathcal{A}) := \max_{y \in Y} \sup_{x \in A_y} \rho(x, y). \tag{4.2}$$

**Theorem 4.1.** *Assume that the bounded linear operator $\Phi : \ell^\infty(\mathcal{X}) \to \Pi_{N_\tau}$ preserves the polynomials from $\Pi_N$. Let*

$$q := d(\mathcal{A}) N_\tau \|\Phi\| < 1. \tag{4.3}$$

*Set $\mathcal{R} = (\mathcal{I} - \mathcal{E}_{\mathcal{A}})\Phi$, where $\mathcal{I}$ denotes the identity. Then for any $f \in \Pi_N$*

$$f = \sum_{k=0}^{\infty} \mathcal{R}^k(\mathcal{E}_{\mathcal{A}} f) \tag{4.4}$$

*with the series converging uniformly and*

$$\Big\| f - \sum_{k=0}^{n-1} \mathcal{R}^k(\mathcal{E}_{\mathcal{A}} f) \Big\|_{\infty} \le q^n \|f\|_{\infty}, \quad n \ge 1. \tag{4.5}$$

*Proof.* We proceed quite as in the proof of Theorem 2.1. For $f \in \Pi_N$ and $k \ge 0$ we use that $\Phi f = f$ to write

$$\mathcal{R}^k f - \mathcal{R}^{k+1} f = \mathcal{R}^k(f - (\mathcal{I} - \mathcal{E}_{\mathcal{A}})\Phi f) = \mathcal{R}^k(f - f + \mathcal{E}_{\mathcal{A}} f) = \mathcal{R}^k(\mathcal{E}_{\mathcal{A}} f). \tag{4.6}$$

Hence

$$f - \sum_{k=0}^{n-1} \mathcal{R}^k(\mathcal{E}_{\mathcal{A}} f) = \mathcal{R}^n f, \quad \forall f \in \Pi_N. \tag{4.7}$$

We now estimate $\|\mathcal{R}\|$. Clearly

$$\mathcal{R}g(x) = \Phi g(x) - \mathcal{E}_{\mathcal{A}}\Phi g(x) = \Phi g(x) - \Phi g(y_x) \quad \text{for } g \in L^{\infty}(\mathbb{S}^2),\ x \in \mathbb{S}^2.$$

The restriction of $\Phi g$ to the big circle connecting $x$ and $y_x$ is a trigonometric polynomial of degree $N_\tau$ and, therefore, the mean-value theorem and the Bernstein inequality yield

$$|\mathcal{R}g(x)| \le \rho(x, y_x) N_\tau \|\Phi g\|_{\infty} \le d(\mathcal{A}) N_\tau \|\Phi\| \|g\|_{\infty}.$$

Hence

$$\|\mathcal{R}\| \le d(\mathcal{A}) N_\tau \|\Phi\|. \tag{4.8}$$

Now (4.8) and (4.3) give $\|\mathcal{R}\| \le q$, which implies the uniform convergence of the series in (4.4). The last inequality coupled with (4.7) implies (4.5), yielding (4.4). □

Theorem 4.1 provides an exact reconstruction algorithm for $f \in \Pi_N$. Indeed, pick a $(2+\tau)N-$*regular* point set $\mathcal{X} \subset \mathbb{S}^2$ and set $\Phi := \Phi_N$ with $\Phi_N$ being the operator from (3.3). Denote briefly $g_k = \mathcal{R}^k(\mathcal{E}_{\mathcal{A}} f)$. Then Theorem 4.1 implies

$$f(\xi) = \sum_{k=0}^{\infty} g_k(\xi), \quad \xi \in \mathcal{X}, \tag{4.9}$$

which solves Problem 2, and the solution $f(z) = \Phi_N f(z)$ of Problem 3 gives exact reconstruction of $f$ at every $z \in Z \subset \mathbb{S}^2$. Observe that the values $g_k(\xi)$, $\xi \in \mathcal{X}$, can be recursively computed by $g_0(\xi) = f(y_\xi)$ and

$$g_{k+1}(\xi) = \mathcal{R}g_k(\xi) = \Phi_N g_k(\xi) - \Phi_N g_k(y_\xi). \tag{4.10}$$

Note that the evaluation of $\Phi_N g(x)$ by (3.3) uses only the values $g(\xi)$ for $\xi \in \mathcal{X}$.

Of course, for practical purposes we truncate the series in (4.9) to obtain the approximation

$$f(\xi) \approx \sum_{k=0}^{n-1} g_k(\xi),$$

where $n$ is determined by the target accuracy via (4.5).

The complexity of this algorithm is as follows. To determine the $y_\xi$'s one needs $O(|\mathcal{X}|+|Y|)$ operations using that $\mathcal{X}$ is *structured*. Every step in (4.10) requires $O(|\mathcal{X}|^2)$ operations if $\mathcal{K}_N(u)$ can be evaluated with $O(1)$ operations within the machine precision. Thus, the algorithm evaluates $f(\xi)$, $\xi\in\mathcal{X}$, with accuracy $\varepsilon$ using $O(|\mathcal{X}|^2\ln(1/\varepsilon)/\ln(1/q)+|Y|)$ operations.

4.3. **Approximate solution of Problem 2.** As already mentioned the regular point sets from §3.1 have the deficiency that the points in each of them concentrate around the poles or the images of the poles via some rotation. This drawback along with the fact that the value of $\Phi_N f(x)$ is obtained by $O(|\mathcal{X}|)$ operations makes the sampling algorithm from §4.2 impractical. To overcome the second deficiency we shall use the truncated version $\Phi_{N,\delta}$ of the operator $\Phi_N$ defined in (3.5), and to remedy the first deficiency we shall utilize the rotated version $\tilde\Phi_{N,\delta}$ of $\Phi_{N,\delta}$ for the regions around the poles. In this way we will decrease substantially the algorithm's computational cost outlined at the end of Subsection 4.2.

To realize these ideas we first introduce some notation. Given $N\in\mathbb{N}$ and $\varepsilon>0$ (to be determined) we assume that $\mathcal{X}\subset\mathbb{S}^2$ is one of the $M$-regular set points $\mathcal{X}^{(1)}$, $\mathcal{X}^{(2)}$, or $\mathcal{X}^{(3)}$ from §3.1 with $M:=\lceil(2+\tau)N\rceil$. In fact, to us the best choice is $\mathcal{X}:=\mathcal{X}^{(3)}$.

Let $\delta>0$ be a constant such that (3.6) holds and let $\Phi_{N,\delta}$ be the operator defined in (3.5) . We subdivide $\mathbb{S}^2$ into two: The equatorial area (belt) $\mathcal{U}_1$ and its compliment (the polar regions) $\mathcal{U}_2$, defined in spherical coordinates by

$$\mathcal{U}_1:=\{x\in\mathbb{S}^2:\pi/4\le\theta\le 3\pi/4\},\quad \mathcal{U}_2:=\mathbb{S}^2\setminus\mathcal{U}_1. \tag{4.11}$$

We also introduce the following sets of nodes on $\mathbb{S}^2$:

$$\begin{aligned}&\mathcal{X}_1:=\mathcal{X}\cap\{\pi/4-\delta_0\le\theta\le 3\pi/4+\delta_0\},\\ &\mathcal{X}_2:=T(\mathcal{X})\cap(\{0\le\theta\le\pi/4+\delta_0\}\cup\{3\pi/4-\delta_0\le\theta\le\pi\}),\\ &\mathcal{X}_0:=\mathcal{X}_1\cup\mathcal{X}_2,\end{aligned} \tag{4.12}$$

where $\delta_0:=\delta+d(\mathcal{A})$. We assume $\delta_0<\pi/4$.

We now introduce the linear operator

$$\mathcal{R}g(x):=(\mathcal{I}-\mathcal{E}_\mathcal{A})\Phi_{N,\delta}g(x)\cdot\mathbb{1}_{\mathcal{U}_1}(x)+(\mathcal{I}-\mathcal{E}_\mathcal{A})\tilde\Phi_{N,\delta}g(x)\cdot\mathbb{1}_{\mathcal{U}_2}(x). \tag{4.13}$$

The above operator only uses the values of $g$ at the points of $\mathcal{X}_0$. Indeed, if $x\in\mathcal{U}_1$ then $\mathcal{E}_\mathcal{A}\Phi_{N,\delta}g(x)=\Phi_{N,\delta}g(y_x)$ uses the values $g(\xi)$ for $\xi\in\mathcal{X}$ and $\rho(y_x,\xi)\le\delta$, hence $\rho(x,\xi)\le\delta+d(\mathcal{A})$, i.e. $\xi\in\mathcal{X}_1$. Let us point out that for these $x$ the value of $\Phi_{N,\delta}g$ at $y_x$ is determined by the values of $g$ at $\mathcal{X}_1$ even in the case when $y_x$ itself belongs to $\mathcal{U}_2$. Similar considerations holds for $x\in\mathcal{U}_2$.

Our algorithm for approximate solution of Problem 2 is contained in the following

**Theorem 4.2.** *Assume that* (3.6) *or* (3.9) *holds for some $\varepsilon>0$ and $0<\delta<\pi$. Using the notation from above assume also that*

$$q:=d(\mathcal{A})N_\tau\|\Phi_N\|+2\varepsilon<1. \tag{4.14}$$

*Then for any $f:Y\to\mathbb{R}$ the series $\sum_{k=0}^\infty\mathcal{R}^k(\mathcal{E}_\mathcal{A}f)$ converges uniformly and for any $f\in\Pi_N$*

$$\Big\|f-\sum_{k=0}^{n-1}\mathcal{R}^k(\mathcal{E}_\mathcal{A}f)\Big\|_\infty\le\Big(q^n+\frac{2\varepsilon}{1-q}\Big)\|f\|_\infty. \tag{4.15}$$

*Proof.* We first estimate the norm of the operator $\mathcal{R}$. By (4.13) we have for any function $g : Y \mapsto \mathbb{R}$ and $x \in \mathcal{U}_1$

$$\begin{aligned}\mathcal{R}g(x) &= \Phi_{N,\delta}g(x) - \Phi_{N,\delta}g(y_x)\\ &= \Phi_N g(x) - \Phi_N g(y_x) + (\Phi_{N,\delta} - \Phi_N)g(x) - (\Phi_{N,\delta} - \Phi_N)g(y_x).\end{aligned}$$

Now just as in the proof of Theorem 4.1 we get

$$|\Phi_N g(x) - \Phi_N g(y_x)| \le \rho(x, y_x)N_\tau\|\Phi_N\|\|g\|_\infty \le d(\mathcal{A})N_\tau\|\Phi_N\|\|g\|_\infty$$

and by Proposition 3.1

$$|(\Phi_{N,\delta} - \Phi_N)g(x)| \le \varepsilon\|g\|_\infty, \quad |(\Phi_{N,\delta} - \Phi_N)g(y_x)| \le \varepsilon\|g\|_\infty.$$

Putting the above together we arrive at

$$|\mathcal{R}g(x)| \le (d(\mathcal{A})N_\tau\|\Phi_N\| + 2\varepsilon)\,\|g\|_\infty.$$

Exactly in the same way, using $\tilde\Phi_{N,\delta}$, $\tilde\Phi_N$ instead of $\Phi_{N,\delta}$, $\Phi_N$ we obtain the same estimate for $x \in \mathcal{U}_2$. Therefore,

$$\|\mathcal{R}\| \le d(\mathcal{A})N_\tau\|\Phi_N\| + 2\varepsilon = q. \tag{4.16}$$

The uniform convergence of $\sum_{k=0}^\infty \mathcal{R}^k(\mathcal{E}_\mathcal{A}f)$ follows from (4.16) and (4.14).

Let $f \in \Pi_N$. Clearly,

$$\mathcal{R}^k f - \mathcal{R}^{k+1}f = \mathcal{R}^k(f - \mathcal{R}f) = \mathcal{R}^k(\mathcal{E}_\mathcal{A}f) + \mathcal{R}^k(f - \mathcal{E}_\mathcal{A}f - \mathcal{R}f), \quad k \ge 0,$$

and iterating this identity we obtain

$$f - \sum_{k=0}^{n-1}\mathcal{R}^k(\mathcal{E}_\mathcal{A}f) = \mathcal{R}^n f + \sum_{k=0}^{n-1}\mathcal{R}^k(f - \mathcal{E}_\mathcal{A}f - \mathcal{R}f). \tag{4.17}$$

By the definition of $\mathcal{R}$ in (4.13) we have for $x \in \mathbb{S}^2$

$$\begin{aligned}f(x) - \mathcal{E}_\mathcal{A}f(x) - \mathcal{R}f(x) = f(x) - f(y_x) &- (\Phi_{N,\delta}f(x) - \Phi_{N,\delta}f(y_x))\cdot\mathbb{1}_{\mathcal{U}_1}(x)\\ &- (\tilde\Phi_{N,\delta}f(x) - \tilde\Phi_{N,\delta}f(y_x))\cdot\mathbb{1}_{\mathcal{U}_2}(x)\end{aligned}$$

and using the fact that $\Phi_N f = f$ and $\tilde\Phi_N f = f$ we infer

$$\begin{aligned}f(x) - \mathcal{E}_\mathcal{A}f(x) - \mathcal{R}f(x) = [(\Phi_N - \Phi_{N,\delta})f(x) &- (\Phi_N - \Phi_{N,\delta})f(y_x)]\cdot\mathbb{1}_{\mathcal{U}_1}(x)\\ &+ [(\tilde\Phi_N - \tilde\Phi_{N,\delta})f(x) - (\tilde\Phi_N - \tilde\Phi_{N,\delta})f(y_x)]\cdot\mathbb{1}_{\mathcal{U}_1}(x),\end{aligned}$$

which can be written in the form

$$f - \mathcal{E}_\mathcal{A}f - \mathcal{R}f = (\mathcal{I} - \mathcal{E}_\mathcal{A})(\Phi_N - \Phi_{N,\delta})f\cdot\mathbb{1}_{\mathcal{U}_1} + (\mathcal{I} - \mathcal{E}_\mathcal{A})(\tilde\Phi_N - \tilde\Phi_{N,\delta})f\cdot\mathbb{1}_{\mathcal{U}_2}.$$

We now use (3.6)–(3.7) to obtain

$$\|f - \mathcal{E}_\mathcal{A}f - \mathcal{R}f\|_\infty \le 2\varepsilon\|f\|_\infty. \tag{4.18}$$

Combining this with (4.17) and (4.16) yields (4.15). □

We next explain how the sampling (reconstruction) algorithm based on Theorem 4.2 works. We are given the values $f(y)$, $y \in Y$, of a band-limited function $f \in \Pi_N$. We only need to compute the values $f(\xi)$ at the points $\xi \in \mathcal{X}_0 = \mathcal{X}_1 \cup \mathcal{X}_2$. Then the algorithm for solving Problem 3 enables us to compute the values $f(z)$ at the points $z \in Z$ for an arbitrary set $Z \subset \mathbb{S}^2$.

Denote briefly $g_k := \mathcal{R}^k(\mathcal{E}_\mathcal{A} f)$ with $\mathcal{R}$ defined in (4.13) and $\mathcal{E}_\mathcal{A}$ from (4.1). The values $f(\xi)$ are approximated by

$$f(\xi) \approx \sum_{k=0}^{n-1} g_k(\xi), \quad \xi \in \mathcal{X}_0. \tag{4.19}$$

The gist of our method is that the values $g_k(\xi)$, $\xi \in \mathcal{X}_0$, can be computed recursively. More explicitly, we start from $g_0(\xi) = \mathcal{E}_\mathcal{A} f(\xi) = f(y_\xi)$, $\xi \in \mathcal{X}_0$, and for $k = 0, 1, \dots, n-2$,

$$g_{k+1}(\xi) = \mathcal{R} g_k(\xi) = \Phi_{N,\delta} g_k(\xi) - \Phi_{N,\delta} g_k(y_\xi) \quad \text{if } \xi \in \mathcal{X}_0 \cap \mathcal{U}_1 \tag{4.20}$$

and

$$g_{k+1}(\xi) = \mathcal{R} g_k(\xi) = \tilde{\Phi}_{N,\delta} g_k(\xi) - \tilde{\Phi}_{N,\delta} g_k(y_\xi) \quad \text{if } \xi \in \mathcal{X}_0 \cap \mathcal{U}_2. \tag{4.21}$$

Observe that identities (4.20)–(4.21) are in fact local – the evaluation of $g_{k+1}(\xi)$ involves only the values $g_k(\eta)$ for $\eta$ satisfying $\rho(\eta, \xi) \le \delta + d(\mathcal{A})$. Therefore, the evaluation of $g_{k+1}(\xi)$ for $\xi \in \mathcal{X}_0 \cap \mathcal{U}_1$ involves only points $\eta \in \mathcal{X}_1$ and the evaluation of $g_{k+1}(\xi)$ for $\xi \in \mathcal{X}_0 \cap \mathcal{U}_2$ involves only points $\eta \in \mathcal{X}_2$.

**Remark 4.1.** The series in Theorem 4.2 converges to a function $g \in L^\infty$ which is in general different from the polynomial $f$ but satisfies $\|f - g\|_\infty \le \frac{2\varepsilon}{1-q} \|f\|_\infty$.

**Remark 4.2.** The "remainder" operators $\mathcal{R}$ in Theorem 4.1 can be replaced by $\mathcal{R}_\star = \Phi(\mathcal{I} - \mathcal{E}_\mathcal{A})$. Then Theorem 4.1 remain valid with (4.5) replaced by

$$\Big\| f - \sum_{k=0}^{n-1} \mathcal{R}_\star^k (\Phi \mathcal{E}_\mathcal{A} f) \Big\|_\infty \le q^n \|\Phi\| \|f\|_\infty.$$

The proof is carried out along the lines of the proof of Theorem 4.1 using the identity $\mathcal{R}_\star^k \Phi = \Phi \mathcal{R}^k$. The advantage of this representation is that we approximate $f$ by polynomials (because the partial sums of the series belong to $\Pi_{N_\tau}$) and the price we pay is that the error estimate is worsen by the factor $\|\Phi\| > 1$.

A similar observation applies to Theorem 4.2, where we can replace $\mathcal{R}$ by $\mathcal{R}_\star$ defined by

$$\mathcal{R}_\star g(x) := \Phi_{N,\delta}(\mathcal{I} - \mathcal{E}_\mathcal{A}) g(x) \cdot \mathbb{1}_{\mathcal{U}_1}(x) + \tilde{\Phi}_{N,\delta}(\mathcal{I} - \mathcal{E}_\mathcal{A}) g(x) \cdot \mathbb{1}_{\mathcal{U}_2}(x)$$

and (4.15) by

$$\Big\| f - \sum_{k=0}^{n-1} \mathcal{R}_\star^k (\Phi_{N,\delta} \mathcal{E}_\mathcal{A} f) \Big\|_\infty \le \Big( q^n + \frac{2\varepsilon}{1-q} \Big) \|\Phi_{N,\delta}\| \|f\|_\infty.$$

**Remark 4.3.** Note that the smaller $q$ the faster the convergence in (4.4) or in (4.15). Turning our attention to (4.3) or (4.14) we observe that the smallest $d(\mathcal{A})$ is realized whenever $\mathcal{A}$ is the Voronoi tessellation of $\mathbb{S}^2$ induced by $Y$. Instead of (4.1) one can use other extension operators, e.g. local interpolation.

**Remark 4.4.** The norm $\|\Phi_N\|$ plays an essential role in conditions (4.3) and (4.14). This norm has been computed numerically for various values of $\tau$ and $\varepsilon$ and the results are displayed in Table 6 in Subsection 6.2. For example, if $\tau = 1$ and $\varepsilon = 10^{-5}$, then $\|\Phi_N\| \approx 4.2324$, which implies that the condition $d(\mathcal{A})N < 1/9$ is sufficient for successful reconstruction of spherical polynomials of degree $N$ with relative error $\varepsilon = 10^{-5}$ (or smaller error if $\delta$ is increased). For comparison, the similar sufficient condition in [9, Theorem 1] in our notations reads $d(\mathcal{A})N < 1/308$.

Therefore, our condition on the sampling set $Y$ is a lot more relaxed than the condition given in [9].

## 5. Approximate reconstruction algorithm

Assume in Problem 2 we would like to find the approximate values $F(\xi)$ to the unknown values $f(\xi)$, $\xi \in \mathcal{X}_0$, with absolute error $\varepsilon_0$, i.e. $|F(\xi) - f(\xi)| \le \varepsilon_0$. We determine the relative error $\varepsilon_1 = \varepsilon_0/\|f\|_{\ell^\infty(Y)}$ and split it into two parts $\varepsilon_1 = \varepsilon_2 + 2\varepsilon/(1-q)$, where $\varepsilon_2$ will be the iteration accuracy and $\varepsilon$ – the needlet accuracy.

Here we describe our *algorithm for approximate reconstruction*. If we consider Problem 2 as a step in the solution of Problem 1, then we are free to chose the regular set $\mathcal{X}_0$ from (4.12) in Subsection 4.3. This case is described below. In the case of fixed $\mathcal{X}_0$ in Problem 2 step (1) from the *Pre-computation* part has to be moved to the *Input* part.

*Input*:

(1) Values $f(y)$, $y \in Y$, at an irregular sampling set $Y$.
(2) Degree $N$ of $f$, the cutoff parameter $\tau$, the target relative accuracy $\varepsilon_1$, the iteration accuracy $\varepsilon_2$ and the needlet accuracy $\varepsilon$.

*Pre-computation*:

(1) Compute the number of knots $K$, $L$ so that the cubature be exact for polynomials of degree $M-1$ with $M = \lceil (2+\tau)N \rceil$.
(2) Compute the knots and weights of the one-dimensional quadratures.
(3) Compute the nodes of a regular set $\mathcal{X} = \mathcal{X}^{(3)}$ (see Subsection 3.1).
(4) Compute the weights $w_\xi$ of the cubature (3.1) as tensor product of the one-dimensional quadratures weights.
(5) For every $\xi \in \mathcal{X} \cup T(\mathcal{X})$ find the closest point $y_\xi$ in $Y$.
(6) Compute $\delta$ for the given $N, \varepsilon, \tau$ and a cutoff function $\varphi$ from (3.11)–(3.12).
(7) Compute the values $\varphi(k/N)$ for the given $N, \varepsilon, \tau$ and $\varphi$ from (3.11)–(3.12).
(8) Compute $\mathcal{K}_N(\cos t_r^*)$, $r = -s, -s+1, \dots, R+s$ with downward Clenshaw recurrence (see [8, Subsection 3.3]).
(9) Compute $d = \max_{\xi \in \mathcal{X}} \rho(\xi \cdot y_\xi)$ and form the sets $\mathcal{X}_i$, $i = 0, 1, 2$, with parameter $\delta_0 = \delta + d$ (see (4.12)).
(10) Compute the matrices:
$V^{(1)} = \{v^{(1)}_{\xi,\eta} : \xi \in \mathcal{X}_1 \cap \mathcal{U}_1, \eta \in \mathcal{X}\}$, $V^{(2)} = \{v^{(2)}_{\xi,\eta} : \xi \in \mathcal{X}_2 \cap \mathcal{U}_2, \eta \in T(\mathcal{X})\}$,
$V^{(3)} = \{v^{(3)}_{\xi,\eta} : \xi \in \mathcal{X}_1 \cap \mathcal{U}_2, \eta \in T(\mathcal{X})\}$, $V^{(4)} = \{v^{(4)}_{\xi,\eta} : \xi \in \mathcal{X}_2 \cap \mathcal{U}_1, \eta \in \mathcal{X}\}$,
defined by

$$\begin{aligned} v^{(j)}_{\xi,\eta} &= w_\eta(\widetilde{\mathcal{K}}_N(\xi \cdot \eta) - \widetilde{\mathcal{K}}_N(y_\xi \cdot \eta)), \quad j = 1, 4, \\ v^{(j)}_{\xi,\eta} &= \widetilde{w}_\eta(\widetilde{\mathcal{K}}_N(\xi \cdot \eta) - \widetilde{\mathcal{K}}_N(y_\xi \cdot \eta)), \quad j = 2, 3, \end{aligned} \tag{5.1}$$

where $\widetilde{\mathcal{K}}_N(t) = \mathcal{K}_N(t)$ for $t \ge \cos\delta$ and $\widetilde{\mathcal{K}}_N(t) = 0$ for $t < \cos\delta$.

*Iterations*:

(1) Initial values: $g_0(\xi) = f(y_\xi), F(\xi) = g_0(\xi), \xi \in \mathcal{X}_0$.
(2) Iteration steps: For $k = 0, 1, \dots$ do
(a)

$$g_{k+1}(\xi) = \sum_{\eta \in \mathcal{X}_1} v^{(1)}_{\xi,\eta} g_k(\eta), \ \xi \in \mathcal{X}_1 \cap \mathcal{U}_1; \tag{5.2}$$

(b)

$$g_{k+1}(\xi) = \sum_{\eta\in\mathcal{X}_2} v^{(2)}_{\xi,\eta} g_k(\eta),\ \xi\in\mathcal{X}_2\cap\mathcal{U}_2; \tag{5.3}$$

(c)

$$g_{k+1}(\xi) = \sum_{\eta\in\mathcal{X}_2} v^{(3)}_{\xi,\eta} g_k(\eta),\ \xi\in\mathcal{X}_1\cap\mathcal{U}_2; \tag{5.4}$$

(d)

$$g_{k+1}(\xi) = \sum_{\eta\in\mathcal{X}_1} v^{(4)}_{\xi,\eta} g_k(\eta),\ \xi\in\mathcal{X}_2\cap\mathcal{U}_1; \tag{5.5}$$

(e) $F(\xi) = F(\xi) + g_{k+1}(\xi), \xi\in\mathcal{X}_0$;

(3) Stopping criterion: $\|g_{k+1}\| \le \varepsilon_2\|g_0\|$.

*Output*: The approximate values $F(\xi)$ of $f(\xi)$ at all points $\xi\in\mathcal{X}_0$.

The only condition which has to be met for the work of the algorithm is (4.14). Under this condition the algorithm has geometric convergence and we have

**Proposition 5.1.** *Under the assumption of Theorem 4.2 the relative error of the algorithm output is given by*

$$\frac{\|F-f\|_{\ell^\infty(\mathcal{X}_0)}}{\|f\|_{\ell^\infty(Y)}} < \varepsilon_2 + \frac{2\varepsilon}{1-q} = \varepsilon_1, \tag{5.6}$$

$$\max\{\|\Phi_{N,\delta}F - f\|_{\ell^\infty(Y\cap\mathcal{U}_1)}, \|\tilde{\Phi}_{N,\delta}F - f\|_{\ell^\infty(Y\cap\mathcal{U}_2)}\} < \varepsilon_1\|\Phi_{N,\delta}\|\|f\|_{\ell^\infty(Y)}. \tag{5.7}$$

*Proof.* Inequality (5.6) follows from (4.17), (4.16), (4.18) and the Stopping criterion of the *Iterations* part. Inequality (5.7) follows by the same argument if we use the operator $\mathcal{R}_\star$ from Remark 4.2 instead of $\mathcal{R}$. □

Inequality (5.6) shows that the prescribed accuracy is achieved by the algorithm, while (5.7) give us a tool to verify whether the computed values $F(\xi)$, $\xi\in\mathcal{X}_0$, reconstruct the spherical polynomial $f$, known by its values at the scattered points $y\in Y$.

*Complexity of the algorithm.* We determine the complexity for the best choice of $K$ and $L$ in step (1), which means $K = O(N)$, $L = O(N)$. Steps (1), (2), (3), (4), (6), (7), and (8) are analyzed in [8, Subsection 3.7]. In view of the structure condition for regular points in Subsection 3.1 step (5) requires $O(N^2 + |Y|)$ operations. The complexity of step (9) is $O(N^2)$.

Step (10) is the most demanding one on both memory and number of operations (i.e. speed) in the whole algorithm. The "matrices of influence" $V^{(j)}, j = 1,2,3,4$, express the relative distances between the elements of the two sets $\mathcal{X}_0$ and $Y$. Their size is huge: $V^{(1)}$ and $V^{(2)}$ have $O(N^4)$ elements and $V^{(3)}$ and $V^{(4)}$ have $O(N^4\delta_0)$ elements. If one wants to work with the whole "matrices of influence" then polynomial degrees exceeding 200 will be practically prohibitive. For comparison, for degree 1000 we work with a regular set $\mathcal{X}_0$ with close to 6 000 000 points and the nodal sets $\mathcal{X} = \mathcal{X}^{(3)}$ and $T(\mathcal{X})$ have 8 000 000 points each. This makes a total of $4.8\times10^{13}$ elements in the "matrices of influence" and only the storage of such amount of data on a "hard disk" as 8 bytes numbers will require 350 TB of memory!

Using the superb localization of the father needlet kernel $\mathcal{K}_N(x\cdot\xi)$ we make the "matrices of influence" sparse by setting $\widetilde{\mathcal{K}}_N(t)=0$ for $t<\cos\delta$ in (5.1). Thus, the total number of non-zero elements in these matrices is $O(N^2\bar{n})=O(N^4\delta^2)=O(N^2\ln^2(1/\varepsilon))$, where $\bar{n}$ is the average number per point $\xi$ of non-zero elements in (5.1). Several values of $\bar{n}$ are given in Table 1 of Subsection 6.1. For $\tau=2$ they range from 267 for $\varepsilon=10^{-5}$ to 1150 for $\varepsilon=10^{-11}$. Other important parameters of the problem as memory requirements and time of execution are also given in Subsection 6.1. In sum, step (10) requires $O(N^2\ln^2(1/\varepsilon))$ operations but the $O$ constant is quite large.

Every step in the *Iterations* part performs a matrix-times-vector multiplication, where every non-zero element of the "matrices of influence" is used once. This means $O(N^2\ln^2(1/\varepsilon))$ operations. The number of iterations is $\ln(1/\varepsilon_2)/\ln(1/q)$. Hence the choice $\varepsilon_2=\varepsilon_1/3$ and $\varepsilon=(1-q)\varepsilon_1/3$ will give $O(N^2\ln^3(1/\varepsilon_1))$ for the complexity of the algorithm.

*Memory requirements.* For $N=1000$ and $\varepsilon=10^{-7}$ the values of the elements of the sparse "matrices of influence" will occupy some 21 GB memory (see Table 1). With additional 12 GB for the indexes of the non-zero elements we arrive at 33 GB of memory for storage of these matrices. This fact made us decide to save the "matrices of influence" in pieces on the hard disk. Then the operations in (5.2)–(5.5) are executed by reading one piece at a time from HD, performing the multiplication and clearing the matrix piece from the memory before reading a new piece. In this way the execution time for 20 iterations is comparable to the time necessary to compute matrix element values in (5.1) and to save them on HD (see Table 2 in Subsection 6.1).

Each of the other input, work, and output variables as $F$, old and new $g$ (i.e. $g_k$ and $g_{k+1}$), spherical coordinates of the irregular sample points and the polynomial values requires $O(N^2)$ memory. In view of the small number of such variables this is easily manageable for $N$ in the range of several thousand.

*Optimal choice of needlet parameter $\tau$.* For $M=\lceil(2+\tau)N\rceil$, $K=\lceil M/2\rceil$, $L=M$ we have:

- The number of nodes in $\mathcal{X}_0$ is proportional to $M^2$;
- The average number of nodes from $\mathcal{X}_0$ in a $\delta$ neighborhood is proportional to $\delta^2M^2$.

Hence, both the size of the "matrices of influence" and the number of operation in (5.2)–(5.5) for a single iteration step are proportional to $\delta^2M^4$. Using (3.10) we get $\delta^2M^4=O((2+\tau)^4\tau^{-2}N^2)$ and the minimal value of the last expression is attained for $\tau=2$. Therefore, the best choice of the needlet parameter $\tau$ relative to memory usage as well as speed is $\tau=2$.

## 6. Numerical examples

6.1. **Reconstruction.** We have implemented our reconstruction algorithm in a MATLAB R2012b code and have extensively tested it on a 2.4 GHz PC, CPU Intel Core i7 with 16 GB of RAM. The code does not relay on variable precision arithmetic.

For irregular points we have taken the HEALPix pixel centers and their rotations on the sphere.

The optimal speed and memory requirements were achieved for $\tau = 2$ according to the theory. Hence, we report in this subsection results only for this value of the cutoff parameter. In the latitude direction the quadrature is Gaussian.

For $K = 2N$, $L = 4N$ and $\varphi$ from (3.11)–(3.12) we get the following values for the size of the "influence matrices", i.e. number of points in $\mathcal{X}_0$ and average number of non-zero elements in (5.1).

| $N \setminus \varepsilon$ | $10^{-5}$ | $10^{-7}$ | $10^{-9}$ | $10^{-11}$ |
|---|---|---|---|---|
| 250 | 384728 x 270 | 396300 x 494 | 408016 x 786 | 419836 x 1150 |
| 500 | 1470932 x 268 | 1493560 x 488 | 1516332 x 773 | 1539128 x 1127 |
| 1000 | 5749660 x 267 | 5794400 x 485 | 5839244 x 767 | 5884128 x 1117 |

TABLE 1. Size of the "influence matrices": number of points in $\mathcal{X}_0$ and average number of non-zero elements

For different irregular sampling sets $Y$ the average number of non-zero elements may slightly vary. The number of points in $\mathcal{X}_0$ grows slowly when $\varepsilon$ decreases due to the $\log \varepsilon$ enlargement of the adjacent sets $\mathcal{X}_1 \cap \mathcal{U}_2$ and $\mathcal{X}_2 \cap \mathcal{U}_1$.

The polynomial values were provided by several low and high degree polynomials. Among them were the polynomials $G_N$ and $\widetilde{G}_N$ given by

$$\begin{aligned} G_N(\theta,\lambda) :=& \sum_{m=1}^{N} m^{-1/3} q_{m,N} P_{m,N}(\cos\theta)\sin(m\lambda) \\ &+ \sum_{m=1}^{N-3} m^{-1/3} q_{m,N-3} P_{m,N-3}(\cos\theta)\sin(m\lambda), \\ \widetilde{G}_N(\theta,\lambda) :=& q_{0,N} P_{0,N}(\cos\theta) + 2\sum_{m=1}^{N} q_{m,N} P_{m,N}(\cos\theta)\cos(m\lambda), \end{aligned}$$

where $P_{m,n}$ are the associated Legendre functions and the coefficients $q_{m,n}$ are selected so that they normalize to 1 in $L^2(\mathbb{S}^2, \frac{1}{4\pi} d\sigma)$ each spherical harmonic term.

The uniform norms of $G_N$ and $\widetilde{G}_N$ for selected values of $N$ are given in Tables 3 and 4, respectively. The global extrema of $G_N$ and $\widetilde{G}_N$ are localized around the points $(\frac{\pi}{2}, \frac{\pi}{2})$ and $(\frac{\pi}{2}, \frac{3\pi}{2})$. The graph of $G_{100}$ in spherical coordinates is given in Figure 1, while Figure 2 shows a typical behavior of this function in a region away from global extrema. We believe that the polynomials $G_N$ and $\widetilde{G}_N$ are good for testing of our reconstruction algorithm since they have relatively large spherical harmonic coefficients and highly oscillatory behavior.

| Degree $N$ | 250 | 500 | 1000 | 2000 |
|---|---|---|---|---|
| *Pre-computation* part | 6.2 | 23.0 | 92.7 | 363.5 |
| *Iterations* part (20 iterations) | 6.2 | 24.2 | 96.1 | 384.4 |
| Total | 12.4 | 47.2 | 188.8 | 747.9 |

TABLE 2. Execution times (in minutes) of the reconstruction algorithm

Table 2 contains the execution times of the *Pre-computation* and *Iterations* parts of the reconstruction algorithm. The *Pre-computation* time is the total of the times for execution of all steps of *Pre-computation* from Section 5 plus the saving time on HD. The *Iterations* time includes the execution times for all steps of *Iterations* plus the "matrices of influence" loading time from HD. The number of irregular

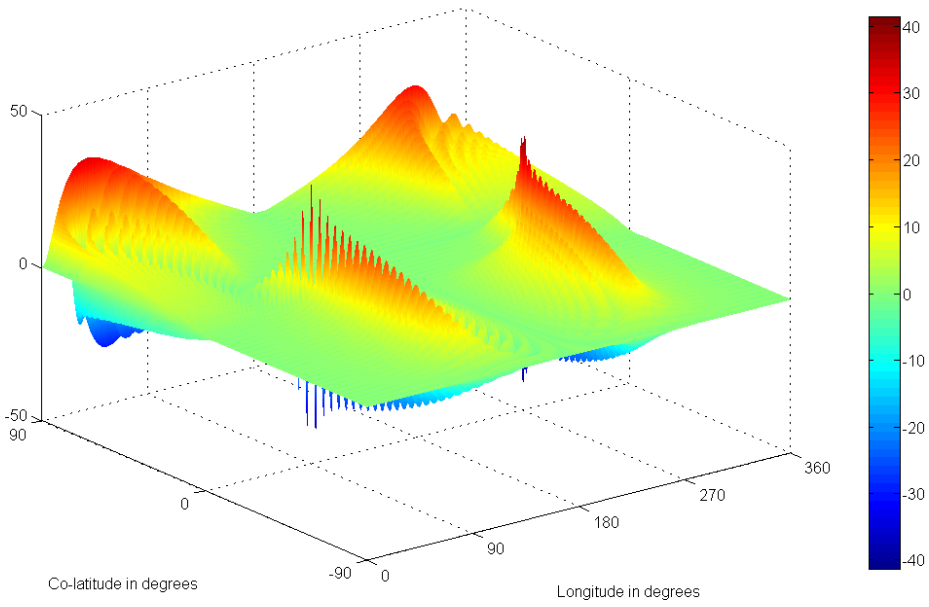


FIGURE 1. Graph of $G_{100}$

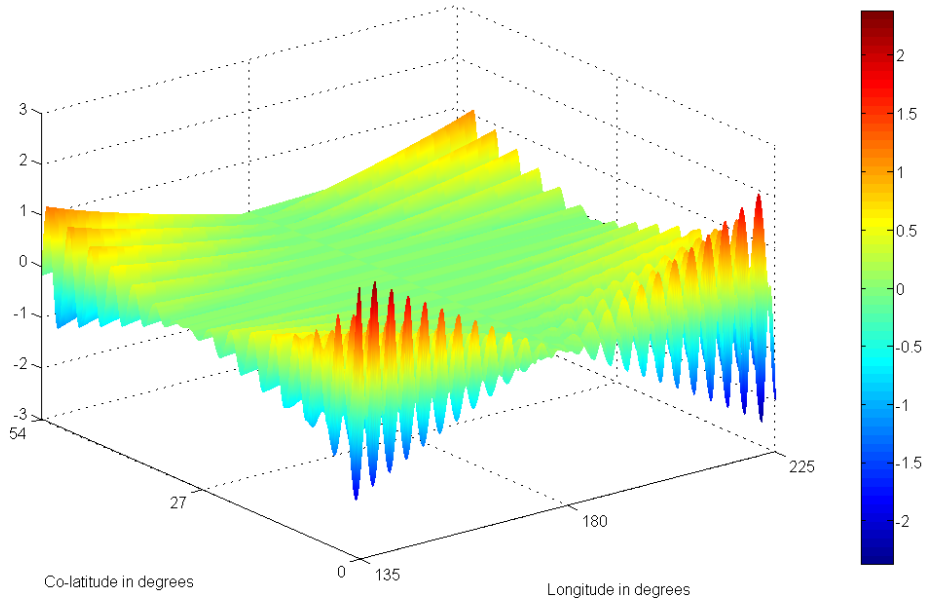


FIGURE 2. Graph of $G_{100}$ over $\{(\theta,\lambda) : \frac{\pi}{5} \le \theta \le \frac{\pi}{2}, |\pi - \lambda| \le \frac{\pi}{4}\}$

sampling points is about 8 times larger than the number of regular points in $\mathcal{X}_0$, but their influence on the times reported below is minimal (apart from the number

of iterations for achieving the target accuracy). The values of the other parameters are $\varepsilon = 10^{-7}$, $K = 2N$, $L = 4N$, and the number of iterations is 20.

We see that the execution times are proportional to $N^2$ according to the theory given in Section 5. The saving time is approximately 27% of the *Pre-computation* time, while the loading time is approximately 63% of the *Iterations* time.

The relative errors defined in (5.6) for $f = G_N$ and $f = \widetilde{G}_N$ at the regular points $\mathcal{X}_0$ are given in Tables 3 and 4, respectively. These errors are obtained from the algorithm from §5 and its modification described in Remark 4.2 with accuracy parameters $\varepsilon = 10^{-7}$ and $\varepsilon_2 = 10^{-8}$.

| Degree $N$ | 250 | 500 | 1000 | 2000 |
|---|---|---|---|---|
| Uniform norm $\|G_N\|_\infty$ | 76.45 | 121.35 | 192.65 | 305.86 |
| Algorithm from §5 | 8.4667e-09 | 7.8133e-09 | 5.7893e-09 | 5.8170e-09 |
| Algorithm from Remark 4.2 | 9.6770e-09 | 1.1789e-08 | 9.2821e-09 | 9.5697e-09 |

TABLE 3. Uniform norms and relative errors from (5.6) for $G_N$

| Degree $N$ | 250 | 500 | 1000 | 2000 |
|---|---|---|---|---|
| Uniform norm of $\|\widetilde{G}_N\|_\infty$ | 480.60 | 958.99 | 1915.4 | 3828.0 |
| Algorithm from §5 | 5.6226e-09 | 5.6581e-09 | 5.4573e-09 | 5.3932e-09 |
| Algorithm from Remark 4.2 | 6.5248e-09 | 6.6718e-09 | 6.0687e-09 | 6.0394e-09 |

TABLE 4. Uniform norms and relative errors from (5.6) for $\widetilde{G}_N$

As a rule the observed relative errors are 10 to 15 times smaller than the target relative accuracy $\varepsilon_1$! Our experiments also show that the relative errors from (5.7) at the sampling points $Y$ are very close to the respective errors at the regular points $\mathcal{X}_0$.

6.2. **Norms of operators.** The operator norms in this subsection are $\infty \to \infty$ norms. The norm of the integral needlet operator (2.9) is given by

$$\|\varphi(N^{-1}\sqrt{L})\| = \sup_{x\in\mathbb{S}^2} \frac{1}{4\pi} \int\limits_{\mathbb{S}^2} |\mathcal{K}_N(x\cdot y)|\, d\sigma(y) = \frac{1}{2}\int\limits_{-1}^{1} |\mathcal{K}_N(t)|\, dt. \tag{6.1}$$

For $\varphi$ from (3.11)–(3.12) and for various $\tau$ and $\varepsilon$ the numerical values of the norm from (6.1) for $N = 40$, $N = 400$, $N = 4000$ are displayed in Table 5.

As Table 5 shows the norm practically does not depend on the degree $N$. This fact is in compliance with the theory which states that these norms have majorants, which are independent of $N$. The slight decrease of the norm with $N$ is predictable and is due to the increased smoothness of the kernel $\mathcal{K}_N$. The variations of the norm with $\tau$ and $\varepsilon$ are due to the different functions $\varphi$ defined in (3.11)–(3.12).

The norms of the discrete operators $\Phi_N$ and $\Phi_{N,\delta}$ are given by

$$\|\Phi_N\| = \sup_{x\in\mathbb{S}^2} \sum_{\xi\in\mathcal{X}} w_\xi |\Phi_N(x\cdot\xi)| \tag{6.2}$$

and

$$\|\Phi_{N,\delta}\| = \sup_{x\in\mathbb{S}^2} \sum_{\substack{\xi\in\mathcal{X}\\ \rho(x,\xi)\le\delta}} w_\xi |\Phi_N(x\cdot\xi)|. \tag{6.3}$$

| $\tau$ | $N \setminus \varepsilon$ | $10^{-5}$ | $10^{-7}$ | $10^{-9}$ | $10^{-11}$ |
|---|---|---|---|---|---|
| 1 | 40 | 3.1364 | 3.4067 | 3.6306 | 3.8230 |
| | 400 | 3.1280 | 3.3996 | 3.6251 | 3.8194 |
| | 4000 | 3.1267 | 3.3982 | 3.6236 | 3.8179 |
| 2 | 40 | 2.4559 | 2.6774 | 2.8613 | 3.0197 |
| | 400 | 2.4487 | 2.6700 | 2.8538 | 3.0123 |
| | 4000 | 2.4478 | 2.6691 | 2.8529 | 3.0114 |
| 3 | 40 | 2.1905 | 2.3927 | 2.5606 | 2.7054 |
| | 400 | 2.1849 | 2.3867 | 2.5545 | 2.6991 |
| | 4000 | 2.1842 | 2.3861 | 2.5538 | 2.6984 |
| 4 | 40 | 2.0510 | 2.2421 | 2.4010 | 2.5380 |
| | 400 | 2.0465 | 2.2373 | 2.3960 | 2.5328 |
| | 4000 | 2.0460 | 2.2368 | 2.3954 | 2.5323 |

TABLE 5. Numerical evaluation of norm from (6.1)

Let us recall that due to (3.7) the two norms are quite close, namely,

$$0 < \|\Phi_N\| - \|\Phi_{N,\delta}\| \leq \varepsilon.$$

The norms in (6.2) and (6.3) depend on $N$, $\delta$, $\varphi$, $\tau$, $\varepsilon$, $K$, $L$, and the type of the regular nodes used. As in the case of the norm in (6.1) the relative variation of these norms with respect to $N$ is less than one percent.

For $N = 500$ and for various $\tau$ and $\varepsilon$ the numerical values of the norm from (6.2) are displayed in Table 6. The other parameters for the computations are: Gaussian quadrature with $K = 2\lceil(2+\tau)N/4\rceil$, $L = 2K$, and $\varphi$ from (3.11)–(3.12).

| $\tau \setminus \varepsilon$ | $10^{-5}$ | $10^{-7}$ | $10^{-9}$ | $10^{-11}$ |
|---|---|---|---|---|
| 1 | 4.2324 | 4.6610 | 5.0166 | 5.3227 |
| 2 | 3.1562 | 3.5077 | 3.7990 | 4.0497 |
| 3 | 2.7355 | 3.0577 | 3.3245 | 3.5540 |
| 4 | 2.5137 | 2.8193 | 3.0724 | 3.2901 |

TABLE 6. Numerical evaluation of $\|\Phi_N\|$ for $\mathcal{X} = \mathcal{X}^{(3)}$

In Theorem 4.2 and in the solution of Problem 3 from [8] instead of $\Phi_{N,\delta}$ we in fact use the operators $\Phi_{N,\delta} \cdot \mathbb{1}_{\mathcal{U}_1} + \tilde{\Phi}_{N,\delta} \cdot \mathbb{1}_{\mathcal{U}_2}$. Their norms are given by

$$\|\Phi_{N,\delta} \cdot \mathbb{1}_{\mathcal{U}_1} + \tilde{\Phi}_{N,\delta} \cdot \mathbb{1}_{\mathcal{U}_2}\| = \sup_{\substack{x \in \mathbb{S}^2 \\ \pi/4 \leq \theta \leq 3\pi/4}} \sum_{\substack{\xi \in \mathcal{X} \\ \rho(x,\xi) \leq \delta}} w_\xi |\Phi_N(x \cdot \xi)|. \tag{6.4}$$

For the same values of the parameters as in Table 6 we have these norms:

| $\tau \setminus \varepsilon$ | $10^{-5}$ | $10^{-7}$ | $10^{-9}$ | $10^{-11}$ |
|---|---|---|---|---|
| 1 | 3.7265 | 4.0423 | 4.3022 | 4.5245 |
| 2 | 2.9159 | 3.1833 | 3.4026 | 3.5898 |
| 3 | 2.5899 | 2.8396 | 3.0438 | 3.2178 |
| 4 | 2.4152 | 2.6549 | 2.8507 | 3.0174 |

TABLE 7. Numerical evaluation of $\|\Phi_{N,\delta} \cdot \mathbb{1}_{\mathcal{U}_1} + \tilde{\Phi}_{N,\delta} \cdot \mathbb{1}_{\mathcal{U}_2}\|$ for $\mathcal{X} = \mathcal{X}^{(3)}$

According to (6.3) and (6.4)

$$\|\Phi_{N,\delta} \cdot \mathbb{1}_{\mathcal{U}_1} + \tilde{\Phi}_{N,\delta} \cdot \mathbb{1}_{\mathcal{U}_2}\| \leq \|\Phi_{N,\delta}\|. \tag{6.5}$$

For the nodes $\mathcal{X} = \mathcal{X}^{(3)}$ generated by the Gaussian quadrature one has strict inequality in (6.5) as evidenced by Tables 6 and 7. The reason for this is that the supremums in (6.2) and (6.3) are attained for $x$ at one of the poles, while the supremum in (6.4) is attained for $x$ at the equator.

For $\mathcal{X} = \mathcal{X}^{(1)}$ or $\mathcal{X} = \mathcal{X}^{(2)}$ all supremums above are attained for $x$'s at the equator and, hence, in (6.5) we have an equality. For these types of nodes and minimal possible $K$ and $L$ the norm values are approximately in the middle between the norm in (6.1) given in Tables 5 and the norm in (6.4) given in Table 7. The main reason for the decrease of the norm is that the number of knots in latitude direction is doubled. The general rule is that for a fixed cutoff function $\varphi$ whenever the nodes get denser then the norm becomes smaller and tends to the value given in Table 5. Note that the parameters $K$ and $L$ are optimized for speed, but not to minimize $\|\Phi_N\|$.

The results in this subsection show that the norms of our needlet-type operators are quite small, which in turn guarantees the stability of the described algorithms.

## References


[1] T. Coulhon, G. Kerkyacharian, P. Petrushev, Heat kernel generated frames in the setting of Dirichlet spaces, J. Fourier Anal. Appl. 18 (2012), 995–1066.

[2] H. Feichtinger, K. Gröchenig, Irregular sampling theorems and series expansions of bandlimited functions, J. Math. Anal. Appl 167 (1992), 530–556.

[3] H. Feichtinger, K. Gröchenig, Iterative reconstruction of multivariate band-limited functions from irregular sampling values, SIAM J. Math. Anal. 231(1992), 244–261.

[4] H. Feichtinger, K. Gröchenig, Theory and Practice of Irregular Sampling, In: Benedetto, J., Frazier M., eds., Wavelets: Mathematics and Applications, pp. 305–363, Stud. Adv. Math., CRC, Boca Raton, FL, 1994.

[5] H. Feichtinger, K. Gröchenig, and T. Strohmer, Efficient numerical methods in nonuniform sampling theory, Numer. Math. 69 (1995), 423–440.

[6] H. Feichtinger, I. Pesensen, Iterative recovery of band-limited functions on manifolds, Contemp. Math. 345 (2004), 137–153.

[7] A. Glaser, X. Liu and V. Rokhlin, A fast algorithm for the calculation of the roots of special functions, SIAM Journal on Scientific Computing, 29 (2007), 1420–1438.

[8] K. G. Ivanov, P. Petrushev, Fast memory efficient evaluation of spherical polynomials at scattered points, preprint. http://imi.cas.sc.edu/papers/

[9] J. Keiner, S. Kunis, and D. Potts, Efficient reconstruction of functions on the sphere from scattered data, J. Fourier Anal. Appl. 13 (2007), 435–458.

[10] G. Kerkyacharian, P. Petrushev, Heat kernel based decomposition of spaces of distributions in the framework of Dirichlet spaces, Trans. Amer. Math. Soc. (to appear).

[11] S. Kunis, D. Potts, Fast spherical Fourier algorithms, J. Comput. Appl. Math. 161 (2003), 75–98.

[12] S. Kunis, D. Potts, Stability results for scattered data interpolation by trigonometric polynomials, SIAM J. Sci. Comput. 29 (2007), 1403–1419.

[13] L. N. Trefethen and others, Chebfun Version 4.2, The Chebfun Development Team, 2011, http://www.maths.ox.ac.uk/chebfun/.



Institute of Mathematics and Informatics, Bulgarian Academy of Sciences, 1113 Sofia, Bulgaria

*E-mail address*: kamen@math.bas.bg

Department of Mathematics, University of South Carolina, Columbia, SC 29208, and Institute of Mathematics and Informatics, Bulgarian Academy of Sciences

*E-mail address*: pencho@math.sc.edu